

## **ACCELERATED ANTENNA DESIGN METHODOLOGY EXPLOITING PARAMETERIZED CAUCHY MODELS**

**G. Shaker**

Electrical and Computer Engineering  
University of Waterloo  
Waterloo, Ontario, Canada

**M. H. Bakr**

Electrical and Computer Engineering  
McMaster University  
Hamilton, Ontario, Canada

**N. Sangary**

Research in Motion Ltd. (RIM)  
University of Waterloo  
Waterloo, Ontario, Canada

**S. Safavi-Naeini**

Electrical and Computer Engineering  
University of Waterloo  
Waterloo, Ontario, Canada

**Abstract**—We propose an optimization methodology suitable for the design of various antenna structures. This methodology includes a rapidly-converging iterative scheme. In each iteration stage, the algorithm generates a parameterized Cauchy model using the available results from previous iterations. Optimization is then applied to this Cauchy model to obtain better design parameters that are also used in enhancing the accuracy of the model. This cycle continues until the specifications are met. In addition, this on-the-fly technique produces an analytical model of the behavior of the antenna structure. Sensitivity and tolerance analysis can thus be efficiently carried out without the need for further costly electromagnetic simulations.

---

Corresponding author: G. Shaker (gshaker@uwaterloo.ca).

## 1. INTRODUCTION

Miniaturized handheld form-factors, wider network coverage, good radio performance, and higher integration of features come together to define our expectations of a modern wireless communication system. In any downsized wireless device, antennas play the role of its physical sensors, interfacing the device to the outer world. To fulfill their role, these antennas have to be small enough and meet strict system specifications. With the requirement for various form-factor designs and coverage over numerous wireless communication bands, different antenna designs are essential. This motivates research for robust and efficient design methodologies.

In most cases, the package-integrated antenna design is too complex. Analytical methods can not fully produce an antenna performing as required. On the other hand, simple cut-and-try on-the-bench approaches can be time consuming. With the advances in computational power, an alternative route is to design through numerical electromagnetic simulations. Nevertheless, if not guided through efficient design routines, this process could also become quite costly.

Combining electromagnetic simulations with powerful optimization routines represents the heart of many Computer Aided Design (CAD) approaches. Many interesting optimization approaches have been proposed, and some have already become a standard feature in many commercial electromagnetic simulators [1]. Among these are the classical quasi-Newton techniques [2], genetic-based algorithms [3, 4], particle swarm optimization [5–7], evolutionary programming [8–10], and space mapping [11–15]. Some of these algorithms are also integrated with artificial neural networks [16, 17] leading to an efficient design approach.

The motivation of this work is to develop a new antenna design approach that requires fewer calls to the electromagnetic (EM) simulator, and thus results in a faster design cycle. In addition to achieving a feasible design, it is also desirable to assess the antenna sensitivity to fabrication/assembly tolerances without the need for further EM simulations. This motivates research on models that accurately describe the behavior of the designed antenna.

Our proposed approach can be classified as an on-the-fly optimization procedure that does not require a priori knowledge or simulations [18–20]. A multi-dimensional Cauchy model is constructed at each iteration stage using the available EM simulations from previous iterations. The model is then optimized to predict a new design parameter. This new design is accepted if it improves the design

objective function. Otherwise, it is rejected. In all cases, this point is then used, along with all available EM simulations, to construct a more accurate Cauchy model. The updated model is then utilized to predict a better design.

This work is divided as follows: First, a review of the utilized multi-dimensional Cauchy modeling technique is presented in Section 2. Next, we present our proposed design optimization methodology in Section 3. We discuss in detail the flow chart of the algorithm and its different steps. Several examples are then presented in Section 4 which covers different types of antenna structures. Finally, the conclusions are discussed in Section 5.

## 2. MODELING USING MULTI-DIMENSIONAL RATIONAL FUNCTIONS

### 2.1. Notations

Let us consider a general electromagnetic response,  $R(p_1, p_2, \dots, p_n)$ , which is a function of  $n$  parameters,  $p_1, p_2, \dots, p_n$ . These parameters may include frequency, dimensions of different discontinuities, and material properties. We may model such a response by a multidimensional Cauchy rational function in the form:

$$R(p_1, p_2, \dots, p_n) = \frac{N(p_1, p_2, \dots, p_n)}{D(p_1, p_2, \dots, p_n)} = \frac{N(\mathbf{p})}{D(\mathbf{p})} \quad (1)$$

where  $N(p_1, p_2, \dots, p_n)$  and  $D(p_1, p_2, \dots, p_n)$  are polynomial functions of the design parameters. The order of these polynomials is typically determined according to the nature of the problem. In the most general form, the numerator, or the denominator, of order  $M$  with  $N$  parameters, can be written in the form:

$$\left( a_0 + \sum_{i=1}^N a_i p_i \right)^M \quad (2)$$

Through simple manipulations, we can write the number of terms in such a polynomial as:

$$\# \text{ of Terms} = 1 + \sum_{j=1}^M \left( \prod_{i=1}^j \left( \frac{N+i-1}{i} \right) \right) \quad (3)$$

The rational approximation given by (1) was initially utilized for the case of frequency dependent response [21, 22]. For a long time, this approach was limited to modeling the frequency response for a given set of parameters. In the 1970s, the Cauchy mathematical

approach was extended to model multi-dimensional systems for control applications [23]. Later in the last decade, this multi-dimensional approach was also adapted for EM problems [24–28], where the rational polynomials are functions of both the frequency and other design parameters. However, modeling a medium scale EM problem using this approach would typically require numerous full wave EM simulations. In addition, one remaining challenge is how to obtain the coefficients of these polynomials to model resonant structures [28]. This added a considerable amount of complexity to the problem.

The previous approaches [21–28] enforce the rational approximation (1) at a large number of sample points to construct an overdetermined system of equations of the form  $\mathbf{A}\mathbf{d} = \mathbf{v}$ . This system is then solved using least squares. The solution of this system  $\mathbf{d}^*$  is the vector of optimal polynomial coefficients for both the numerator and the denominator that best fit the sample points. Solving such a system, however, presents some noticeable challenges. In [27], the problem formulation is changed to  $\mathbf{A}\mathbf{d} = 0$  rather than  $\mathbf{A}\mathbf{d} = \mathbf{v}$ , to utilize the total least squares method instead of the least squares method. This approach produces good results in low dimensional problems, but suffers from spurious solutions that would lead to a non-physical model [27]. In [24], the multidimensional problem is divided into multiple one dimensional problems that are solved recursively. However, this approach requires a large number of sample points to reach a satisfactory model. Other techniques are found in [28], but these approaches are not proven suitable for rapidly varying responses such as those associated with antenna structures.

## 2.2. The Proposed Cauchy Model

Here, the problem is tackled differently by casting it into a linear programming problem. Let us assume that there are  $N_s$  data samples available, given by  $R_i = R(\mathbf{p}_i)$ ,  $i = 1, 2, \dots, N_s$ . The  $i$ th sample is given in a multidimensional Cauchy model by [29]:

$$\hat{R}_i = \frac{\mathbf{a}^T \mathbf{x}_i}{\mathbf{b}^T \mathbf{y}_i} \quad (4)$$

where  $\mathbf{a} = [a_0 \ a_1 \ \dots \ a_{N_n}]^T$  and  $\mathbf{b} = [b_0 \ b_1 \ \dots \ b_{D_n}]^T$  are the optimizable polynomial coefficients. Note that the Cauchy model (4) is not affected if the numerator and the denominator are scaled by the same factor. The vectors  $\mathbf{x}_i$  and  $\mathbf{y}_i$  are, in general, parameter and frequency dependent vectors. The coefficient vectors  $\mathbf{a}$  and  $\mathbf{b}$  should minimize the error between the actual output data points and the Cauchy model. The corresponding optimization problem can be

written as:

$$\min_{a,b} \left\{ \max_i |\mathbf{b}^T \mathbf{y}_i R_i - \mathbf{a}^T \mathbf{x}_i| \right\} \tag{5}$$

Typically, in any numerical solver, or in a realistic measurement experiment, there exists a tolerance margin for the accuracy of the simulated/measured responses. Including the tolerance margin of the data sample is likely to enhance the robustness of the algorithm. The modified optimization algorithm is thus modified to:

$$\min_{a,b} \left\{ \max_i \left\{ \max_{|\Delta R_i| \leq \varepsilon_i} |\mathbf{b}^T \mathbf{y}_i [R_i + \Delta R_i] - \mathbf{a}^T \mathbf{x}_i| \right\} \right\} \tag{6}$$

where  $\Delta R_i$  is the expected error in the  $i$ th sample with  $|\Delta R_i| < \varepsilon_i$ . One problem with this type of formulation is that it allows for the spurious solution  $\mathbf{a}^T \mathbf{x}_i = \mathbf{b}^T \mathbf{y}_i = 0$ . This solution, observed also in [27], results in a non-physical case. In a linear programming problem, this case can be avoided by adding a set of suitable linear constraints.

For example, and without loss of generality, when modeling the scattering parameters response of passive structures, like antennas, we can write:

$$\min_{a,b} \left\{ \max_i \left\{ \max_{|\Delta S_i| \leq \varepsilon_i} \left| \mathbf{b}^T \mathbf{y}_i [S_i + \Delta S_i] - \mathbf{a}^T \mathbf{x}_i \right| \right\} \right\} \tag{7}$$

To ensure that the numerator is never zero, we add the set of linear constraints:

$$\mathbf{b}^T \mathbf{y}_i \geq 1 \quad i = 1, 2, \dots, N_s \tag{8}$$

Note that because the coefficients of the numerator and the denominator are scalable, any positive number can be used in (8). The second set of linear constraints:

$$\mathbf{a}^T \mathbf{x}_i \geq 0 \quad i = 1, 2, \dots, N_s \tag{9}$$

ensures that the response is larger than or equal to zero. For a passive structure, the scattering parameters are between 0 and 1. Thus, the third set of linear constraints is added:

$$\mathbf{b}^T \mathbf{y}_i \geq \mathbf{a}^T \mathbf{x}_i \quad i = 1, 2, \dots, N_s \tag{10}$$

The assembly of the aforementioned linear constraints is a standard procedure in convex optimization problems. However, in its current form, the objective function in (6) is a non-linear function. Classical linear programming techniques allow for dealing with this problem by introducing an auxiliary variable  $t$  as follows [30, 31]:

$$\min_{a,b,t}$$

Subject to : (11)

$$\max_{|\Delta R_i| \leq \varepsilon_i} \left| \mathbf{b}^T \mathbf{y}_i [R_i + \Delta R_i] - \mathbf{a}^T \mathbf{x}_i \right| \leq t, \quad i = 1, 2, \dots, N_s$$

where the set of constraints can be expanded by adding constraints associated with the physical limitations of the system, as discussed earlier. The current nonlinear constraints can now be made linear by expanding it into the two linear constraints

$$\max_{|\Delta R_i| \leq \varepsilon_i} \left\{ \mathbf{b}^T \mathbf{y}_i [R_i + \Delta R_i] - \mathbf{a}^T \mathbf{x}_i \right\} \leq t \tag{12}$$

and

$$- \min_{|\Delta R_i| \leq \varepsilon_i} \left\{ \mathbf{b}^T \mathbf{y}_i [R_i + \Delta R_i] - \mathbf{a}^T \mathbf{x}_i \right\} \leq t \tag{13}$$

where either (12) or (13) is active for the current sample with  $i = 1, 2, \dots, N_s$ .

For a positive valued response, these two sets of linear constraints can be rewritten as:

$$\mathbf{b}^T \mathbf{y}_i [R_i + \varepsilon_i] - \mathbf{a}^T \mathbf{x}_i \leq t \quad i = 1, 2, \dots, N_s \tag{14}$$

and

$$-\mathbf{b}^T \mathbf{y}_i [R_i + \varepsilon_i] + \mathbf{a}^T \mathbf{x}_i \leq t \quad i = 1, 2, \dots, N_s \tag{15}$$

Now, integrating all the previous steps, we get the following linear convex programming problem for the  $S$  parameters [30]:

$$\min_{a,b,t}$$

Subject to :

$$\begin{aligned} \mathbf{b}^T \mathbf{y}_i [S_i + \varepsilon_i] - \mathbf{a}^T \mathbf{x}_i &\leq t \quad i = 1, 2, \dots, N_s \\ \mathbf{b}^T \mathbf{y}_i [-S_i + \varepsilon_i] + \mathbf{a}^T \mathbf{x}_i &\leq t \quad i = 1, 2, \dots, N_s \\ \mathbf{b}^T \mathbf{y}_i &\geq 1 \quad i = 1, 2, \dots, N_s \\ \mathbf{a}^T \mathbf{x}_i &\geq 0 \quad i = 1, 2, \dots, N_s \\ \mathbf{b}^T \mathbf{y}_i &\geq \mathbf{a}^T \mathbf{x}_i \quad i = 1, 2, \dots, N_s \end{aligned} \tag{16}$$

For a general response with general linear physical constraints, the corresponding linear program is given by

$$\min_{a,b,t}$$

Subject to :  $\mathbf{A} \mathbf{d} \leq \mathbf{v}$

where  $\mathbf{d} = [\mathbf{a}^T \mathbf{b}^T t]^T$  is the vector of unknowns of the linear program. The matrix  $\mathbf{A}$  and the vector  $\mathbf{v}$  are the matrix of parameter coefficients and the vector of right hand side constants of the linear program, respectively. They depend on the physical constraints imposed and the number of available samples.

The linear program (17) can be solved by the simplex method [30,31], which yields the global solution of the problem. A linear program of the form (17) with several hundred unknowns is usually solved in few seconds. It is worth mentioning that there are several available optimization packages for solving such linear programming problem, including MOSEK [32], TOMLAB [33], and MATLAB [34].

### 3. OPTIMIZATION USING MULTI-DIMENSIONAL RATIONAL MODELING

#### 3.1. Previous Optimization Approaches

Most of the previous work that addressed multi-dimensional modeling aimed at utilizing the developed models in optimization. Few points can be observed with this approach. First, a large number of sample points is typically needed [24–28]. For example, the lowest possible number of points reported uses 125 points for modeling a simple resonant three-variable problem [24]. This is considered a costly process, given that if the design invokes 5 parameters instead of 3, the number of required simulations will be around 3125. Large number of points exceeding 1000 was also reported in [26,28]. Another issue with this type of modeling is that it assumes a given domain for the parameters. Enlarging this domain would significantly complicate the process as more points may be needed, especially if resonances occur in this domain. On the other hand, shrinking the domain would result in limited modeling scope, in spite of the considerable number of simulations needed to build it.

Thus, to realize an antenna that should incorporate multiple bands and fits into various miniaturized packages, the model-then-optimize approach, in its current form, is quite costly. It would most likely provide similar (if not inferior) performance to currently available optimization routines used in antenna design. Still, one should emphasize that the model-then-optimize approach has the advantage of providing a parameterized model that can be used in tolerance, statistical and yield analysis.

The approach proposed in this work is to construct a parameterized Cauchy model while simultaneously applying optimization. This approach still maintains the capability of performing tolerance, yield, and statistical analysis. We start by first giving simple one-dimensional and three-dimensional illustrative examples of our approach.

### 3.2. A One-dimensional Example Using the Proposed Approach

To illustrate our approach, we first study a simple one-dimensional example. Assume that we need to find the value of the variable  $p$ , denoted by  $p^*$ , such that  $R(p^*) = 0.5$ . For simplicity, we assume that the function  $R(p)$  represents some unknown system behavior which is best described as  $R(p) = \cos(p)$ . Note that this functional behavior is not known to the designer. Now, from a designer's perspective, very few test values of the variable should be needed to find the value which realizes the desired system response  $R(p^*) = 0.5$ . Hence, the algorithm will take the form of Fig. 1. The designer has to supply some initial guess for the value of the parameter  $p$ , along with parameter bounds, that would typically reflect some physical/fabrication limits, in addition to the required response. In this example, we assume that the solution will be within the domain  $p \in [0, \pi]$ . Also, we assume that the initial guess for  $p$  is  $p_0 = 0.9$ .

Our proposed algorithm runs as follows. First, the algorithm uses the user input,  $p_0$ , to call the numerical solver, or control a physical experiment to obtain  $R(p_0)$ . The extraction set, used to construct the Cauchy model, at the first iteration  $R_{CM}^{(0)}(p)$  is thus  $\Phi^{(0)} = \{0.9\}$ . The order of the Cauchy model is predefined. As discussed earlier, this problem can be casted as a convex linear programming of the form (17) to find the best fit to the available sample points.

Here, the number of samples  $N_s$  is equal to one which is the cardinality of the set  $\Phi^{(0)}$ . The next step in the algorithm is to find a better value for  $p$ . We apply optimization to the Cauchy model  $R_{CM}^{(0)}(p)$  seeking the parameter  $p^*$  that satisfies the specified objective. The obtained design  $p_1 = 1.08$  is then verified through a call to the numerical/EM solver to obtain the corresponding new response  $R(p_1)$ .

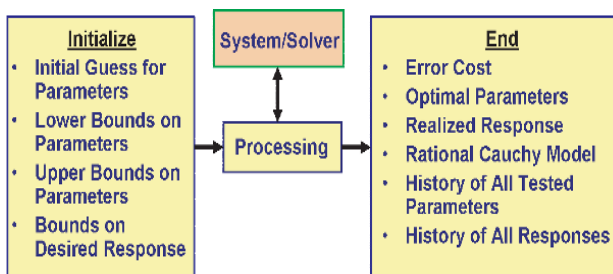


**Figure 1.** A general flow chart of our optimization algorithm.



**Table 1.** Algorithm results starting with  $p_0 = 0.9$ .

Iteration	Parameter Value ( $p$ )	Response Value $R(p)$	Absolute Error
1	0.9	0.6216	0.1216
2	1.08	0.4713	0.0287
3	1.0443	0.5025	0.0025
4	1.0472	0.5000	$2 \times 10^{-6}$

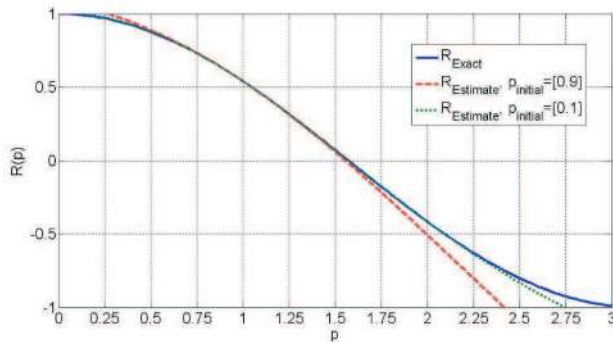


**Figure 2.** A local comparison between the models developed using Cauchy rational functions and the exact response for the one-dimensional example.

The new obtained point is then added to the extraction set to obtain  $\Phi^{(1)} = \{0.9, 1.08\}$ . A new Cauchy rational model  $R_{CM}^{(1)}(p)$  is then constructed using the two available sample points ( $N_s = 2$ ). The cycle goes on till the desired response is achieved. Table 1 illustrates the results obtained for  $p_0 = 0.9$ . Fig. 2 shows how the resulting models behave as a function of the parameter  $p$ . The resulting second order Cauchy model after 4 iterations is:

$$R_{CM}^*|_{p_0=0.9} = 1.088 \frac{1.00 - 0.3918p - 0.1612p^2}{1.00 - 0.1612p + 0.0612p^2} \tag{18}$$

Note that the final Cauchy model is denoted by  $R_{CM}^*(p)$ . It should be emphasized that each iteration stage corresponds to a single call to the numerical/EM solver or to a single physical experiment. Changing the initial point to  $p_0 = 0.1$  results in a comparable accuracy but with a slightly different model:

$$R_{CM}^*|_{p_0=0.1} = 1.021 \frac{1.00 - 0.3361p - 0.1907p^2}{1.00 - 0.2488p + 0.1421p^2} \tag{19}$$

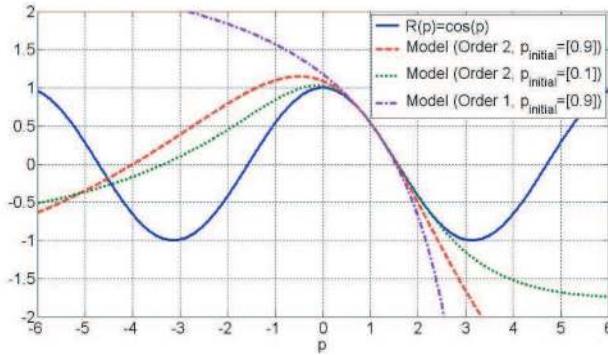


**Figure 3.** A wide range comparison between the models developed using Cauchy rational functions to the exact response for the one-dimensional example.

Changing the order to 1, results in a simpler model but with limited range of accuracy:

$$R_{CM}^*|_{p_0=0.9} = 1.1788 \frac{1.00 - 0.6512p}{1.00 - 0.2394p} \tag{20}$$

Fig. 3 shows a wide range comparison between the Cauchy models of different orders and the exact response. As expected, the models match well within the region of the sample points obtained during optimization. Obvious deviation is noted though outside this region as the Cauchy model was not given any sample points in this region.

### 3.3. A Three-variable Resonance Circuit Using the Proposed Approach

The one-dimensional example illustrates a scenario where we have a simple scalar response. However, resonant structures, such as antennas, are usually modeled over a frequency band. The responses of such resonant-based structures can be approximated by a combination of parallel or series resonance networks. For illustration, we consider an RLC parallel network. The input impedance of such a network is written as:

$$Z_m(\omega, L, C, R) = \frac{1}{\frac{1}{R} + j\omega C + \frac{1}{j\omega L}} \tag{21}$$

The input reflection coefficient seen at the ports of the network can then be written as:

$$S(\omega, L, C, R) = \frac{Z_{in}(\omega, L, C, R) - Z_0}{Z_{in}(\omega, L, C, R) + Z_0} \tag{22}$$

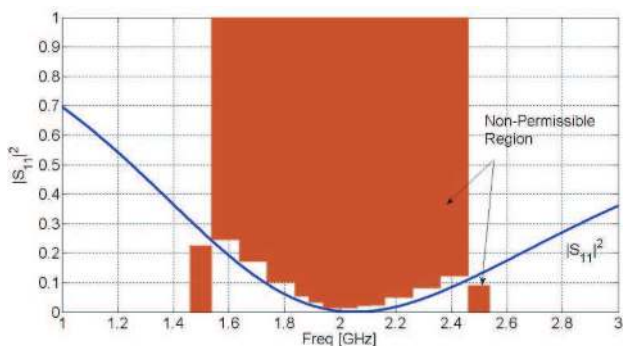


**Figure 4.** The constraints on the three-variable resonance circuit.

where  $Z_0$  is the characteristic impedance of the feed line. After some simple manipulations, we can write:

$$|S(\omega, L, C, R)|^2 = \frac{\left( \begin{matrix} \omega^4 Z_0^2 L^2 C^2 R^2 - 2\omega^2 Z_0^2 L C R^2 + \omega^2 L^2 R^2 \\ -2\omega^2 Z_0 L^2 R + \omega^2 Z_0^2 L^2 + Z_0^2 R^2 \end{matrix} \right)}{\left( \begin{matrix} \omega^4 Z_0^2 L^2 C^2 R^2 - 2\omega^2 Z_0^2 L C R^2 + \omega^2 L^2 R^2 \\ +2\omega^2 Z_0 L^2 R + \omega^2 Z_0^2 L^2 + Z_0^2 R^2 \end{matrix} \right)} \quad (23)$$

In order to accurately model the behavior of this network, we generate a polynomial with the highest powers of both the numerator and denominator. That is, in principle, we need a Cauchy rational function of order 10 to capture all the details of this function. However, in a more realistic design situation, we try to find the values of components, or physical dimensions that realize a given frequency response. For example, Fig. 4 shows a typical desired frequency response where the reflection coefficient at the input ports meets specific constraints.

This simple observation allows us to select few discrete frequencies and include the constraints at each of these frequencies in the convex linear programming algorithm. Thus, the problem simplifies to:

$$|S(L, C, R)|^2 \Big|_{\omega=\omega_{N_f}} = \frac{\left( \begin{matrix} \omega_{N_f}^4 Z_0^2 L^2 C^2 R^2 - 2\omega_{N_f}^2 Z_0^2 L C R^2 + \omega_{N_f}^2 L^2 R^2 \\ -2\omega_{N_f}^2 Z_0 L^2 R + \omega_{N_f}^2 Z_0^2 L^2 + Z_0^2 R^2 \end{matrix} \right)}{\left( \begin{matrix} \omega_{N_f}^4 Z_0^2 L^2 C^2 R^2 - 2\omega_{N_f}^2 Z_0^2 L C R^2 + \omega_{N_f}^2 L^2 R^2 \\ +2\omega_{N_f}^2 Z_0 L^2 R + \omega_{N_f}^2 Z_0^2 L^2 + Z_0^2 R^2 \end{matrix} \right)} \quad (24)$$

We thus create a rational Cauchy model at each frequency of interest. At each frequency, we need to construct a rational Cauchy model of order 6 to capture all the details of the behavior of this function. Hence,

we need to solve for 168 coefficients. However, as illustrated earlier, for design purposes, we do not need to model the full functional behavior. For example, if we use multi-dimensional rational functions of order 3, then we have only 40 coefficients to identify. Here, we specify 13 distinct frequency points, such that the response has to be below a certain value for the 11 middle ones, and higher than a certain value at the edge frequencies as shown in Fig. 5. We can then set up a suitable linear programming problem as discussed earlier.

Following the same previously outlined algorithm, and utilizing a min-max objective function, a third order rational model provides a maximum cost of  $-3 \times 10^{-4}$  deviation at the selected frequencies. The negative sign of the min-max cost function indicates that all constraints are satisfied. It should be emphasized that a third order model requires

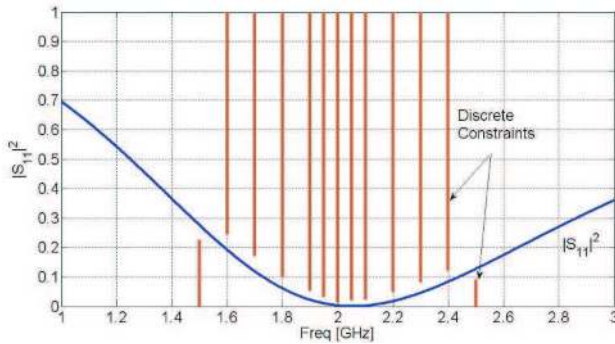


**Figure 5.** The constraints imposed on discrete frequencies of the three-variable resonance circuit.

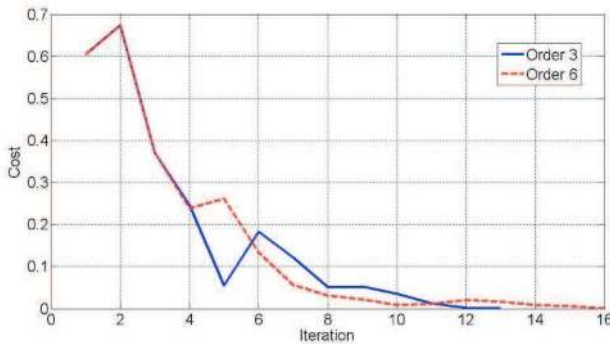


**Figure 6.** The change of the minimax cost function with each iteration for the three-variable resonance circuit.

only 13 calls to the circuit simulator, each with  $R$ ,  $C$ , and  $L$  values as the input parameters. The responses at the thirteen selected frequency points are the corresponding output of the simulator. The same accuracy can be achieved with 16 iterations if we use six-order rational functions as shown in Fig. 6.

It is important to notice the significant acceleration in the achieved results as compared to the “build a complete model then optimize” approach [24–28]. For example, following [24], and assuming 5 points per dimension along with third order rational functions, we would need at least  $4^5 = 1024$  calls to the circuit solver. Optimization would then be carried out exploiting this model to reach the same results that our algorithm reached in only 13 calls.

To assess the potential of the third order model to be used for sensitivity and tolerance analysis, the absolute error between the exact model and the input reflection coefficient  $|S(L, C, R)|$ , calculated from the corresponding third order multidimensional model at 2.0 GHz, is shown in Fig. 7. To perform this calculation, the design parameters are allowed to vary within  $\pm 10\%$  from their nominal value. The included domain is chosen such that  $L \in [1.8, 2.2]$  nH,  $C \in [2.7, 3.3]$  pF, and  $R \in [45, 55]$   $\Omega$ . Each dimension is uniformly divided into 10 points, creating a grid of 1000 points. Fig. 7 shows a histogram of the resulting error calculated at each of the grid points. It is clear that the maximum error is below  $5 \times 10^{-3}$ .

Now, if the variables are allowed to vary by  $\pm 20\%$  from their nominal value, keeping a uniform grid of 1000 points, we get the errors shown in Fig. 8. The error is still relatively small given the allowed percentage change of the parameters.

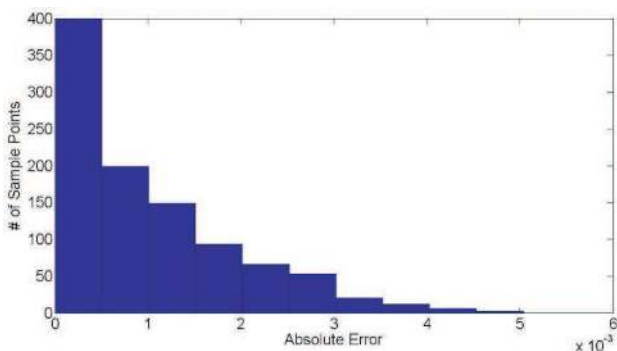


**Figure 7.** The results of the absolute error in tolerance analysis between a 3rd order Cauchy model and actual simulation using a tolerance of 10% for all parameters at 2.0 GHz.

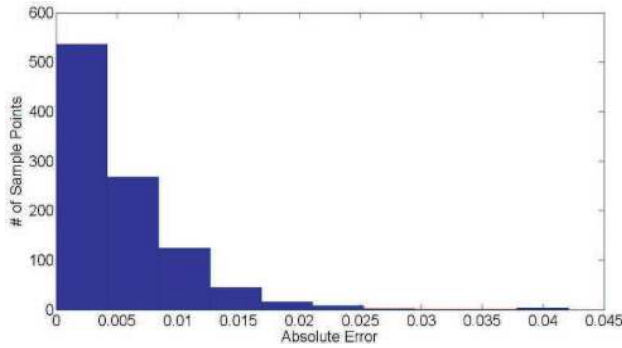


**Figure 8.** The results of the absolute error in tolerance analysis between a 3rd order Cauchy model and actual simulation using a tolerance of 20% for all parameters at 2.0 GHz.

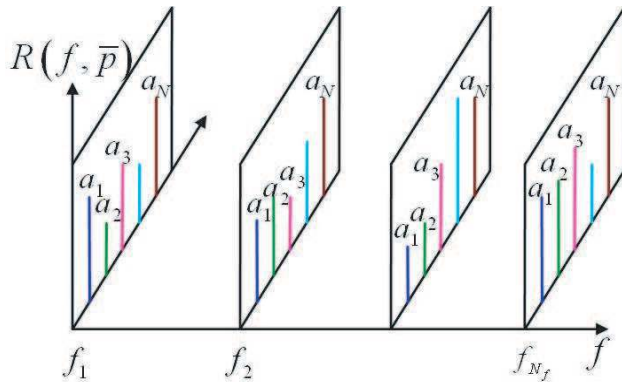


**Figure 9.** The Cauchy coefficients are obtained for a set of discrete frequencies.

So far, we have generated multi-dimensional rational models of a number of parameters at each selected frequency. Fig. 9 illustrates such a situation. It is often desirable, however, to reduce the number of selected frequency points. This speeds up the overall simulation/measurement time and reduces its associated costs. We therefore employ Padé approximation on each of the resulting coefficients to generate frequency dependent coefficients as illustrated in Fig. 10. Using these frequency-dependent coefficients of the multi-dimensional rational model allows us to interpolate and extrapolate rapidly for frequencies other than those selected during the design process.

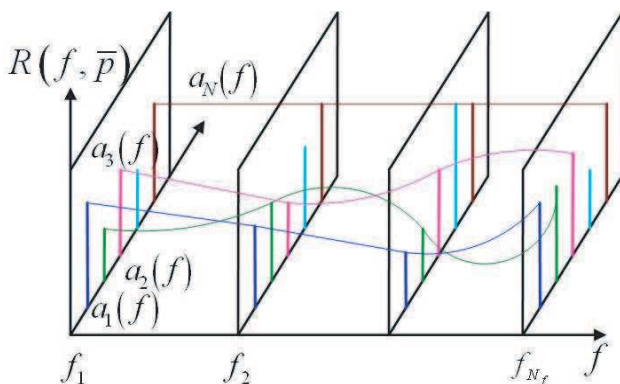


**Figure 10.** The Padé approximation is applied to determine the Cauchy coefficients for frequencies other than the considered ones.

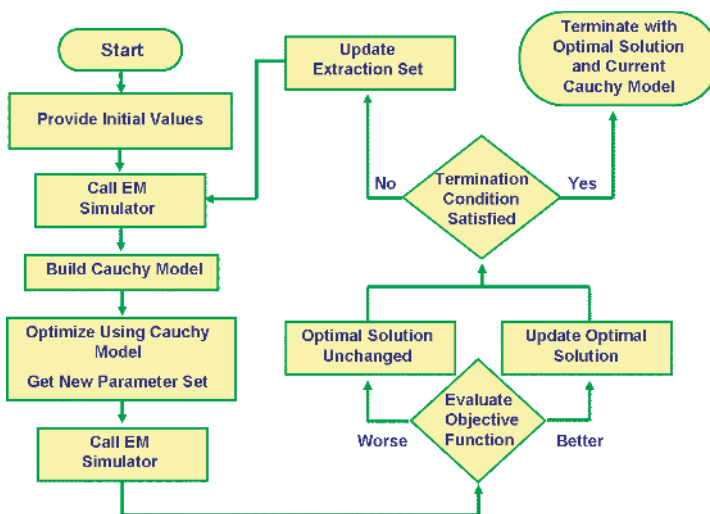


**Figure 11.** The flowchart of the algorithm.

### 3.4. Proposed on-the-fly Optimization Algorithm

The algorithm explained in the previous two illustrative examples can be visualized through the flow chart presented in Fig. 11. The algorithm is summarized in the following steps:

1. Initialization: The iteration counter is set to  $k = 0$ . The starting point  $\mathbf{p}_0$  is given. The extraction set is initialized with  $\Phi^{(0)} = \{\mathbf{p}_0\}$ , with the best available solution initialized with  $\mathbf{p}^* = \mathbf{p}_0$ .

Note that the set  $\Phi^{(k)}$  contains the samples used to construct the Cauchy model in the  $k$ th iteration.

2. The EM simulator is called (or alternatively measurements are carried out) to determine  $R(\mathbf{p}_0)$ .

3. The Cauchy model of the  $k$ th iteration  $R_{CM}^{(k)}(\mathbf{p})$  is constructed using the points in the set  $\Phi^{(k)}$  by solving the linear program (17). Note that a partial set of the points in the set  $\Phi^{(k)}$  may be used in (17) depending on how close the points are to the current iterate  $\mathbf{p}^*$ . As mentioned earlier, constraints could be added to or removed from (17) to fit the considered physical response.

4. The current Cauchy model  $R_{CM}^{(k)}(\mathbf{p})$  is optimized to obtain the new design  $\mathbf{p}_{k+1}$ . A trust region approach [14] is integrated to limit the search for the new design to a region where the Cauchy model is trusted.

5. The response at the new point  $R(\mathbf{p}_{k+1})$  is calculated using EM simulation or measurements.

6. If the new design offers a better objective function, i.e.,  $U(\mathbf{p}_{k+1}) < U(\mathbf{p}^*)$ , then the best available solution  $\mathbf{p}^*$  is set to  $\mathbf{p}_{k+1}$ . Note that  $U$  is the objective function to be minimized during the design process. It may be a least squares or a min-max cost functions depending on the application.

7. If the termination condition is satisfied, the algorithm is terminated, and  $\mathbf{p}^*$  along with the coefficients of the corresponding Cauchy model  $R_{CM}^*(\mathbf{p})$  are reported. The utilized termination condition may include several unsuccessful iterations, or that the iteration counter  $k$  exceeded a certain maximum value.

8. The extraction set is augmented with the new point, i.e.,  $\Phi^{(k+1)} = \Phi^{(k)} \cup \mathbf{p}_{k+1}$ . Set  $k = k + 1$ . The algorithm starts a new iteration from Step 3.

#### 4. EXAMPLES

The proposed algorithm was applied to a number of practical antenna designs. In these designs, the relation between the response and the different parameters is not known. However, as discussed earlier, by selecting an appropriate order for the multidimensional rational polynomials, it is possible to accelerate the design process. In the following examples, the order of the Cauchy model is fixed to 3. With this order, we should be able to locally generate an accurate model that can be used for optimization, sensitivity, and tolerance analyses. The stopping criterion for the algorithm is when the required specifications



are met. We employ the min-max objective function defined by:

$$U(\mathbf{p}) = \max \left\{ R_1^{sign} [R_1 - R_1^{Const}], \dots, R_{N_f}^{sign} [R_{N_f} - R_{N_f}^{Const}] \right\} \quad (25)$$

where  $R_j$  is the actual response at the  $j$ th frequency sample,  $j = 1, 2, \dots, N_f$ . The constraint value  $R_j^{Const}$  denotes the response constraint at the  $j$ th frequency.  $R_j^{sign}$  takes a value of +1 or -1 depending on whether the constraint of the  $j$ th frequency response is an upper or lower constraint, respectively. When all specifications are met, the value of the objective function in (25) should be less than zero.

As discussed earlier, and summarized in Fig. 1, the designer needs to specify the design specifications, the initial guess for the solution, and bounds on the design parameters reflecting typical fabrication limitations or size constraints. All of these are provided to our in-house Matlab-based software. We refer to this code as the Cauchy Engine for Radiators/Resonators (CAUCHER). The core of CAUCHER applies the algorithm as discussed earlier in Section 3. During processing, our software drives the EM solver to reach a valid design. There are several powerful EM solvers available in the market for this purpose. In our algorithm, the CAUCHER software allows the user to choose from a set of solvers, depending on the nature of the problem. After specifying a solver, CAUCHER automatically accesses the EM solver, sets up the design, performs a simulation, retrieves the results, and uses them in the processing cycle (Fig. 11). The EM solvers currently integrated with our CAUCHER software include Ansoft's Designer [36], Ansoft's HFSS [37], COMSOL [38], CST's Microwave Studio [39], Sonnet EM [40], and SPEAG's SEMCAD [41].

To demonstrate the algorithm, several practical antenna designs are presented next. They illustrate the behavior of the algorithm when designing to meet single as well as multiple objectives. Since all of these examples are equally produced by any of the listed EM Solvers, we only list the required number of calls to the solver to reach a feasible design.

#### 4.1. A 3-variable Patch Antenna

The first antenna example addresses the design of a patch antenna [42, 43] such that it meets the constraint  $VSWR \leq 3$  over the band 1.98 GHz–2.04 GHz. The patch should have higher VSWR outside of this band. Thus, by selecting three in-band frequency points, and three out-of-band frequencies, we can define the design specifications as:

$$|S_{11}|^2 = \begin{cases} < 0.25 & \text{In-Band} \\ > 0.25 & \text{Out-of-Band} \end{cases} \quad (26)$$

Here, we use a 3.0 mm thick FR-4 substrate. In addition, we fix the feed point to be on the centre line of the rectangular patch. Thus, we consider three variables for the design. They are the length of the patch  $L_p$ , the width of the patch  $W_p$ , and the feed distance from one edge  $x_f$  (See Fig. 12).

Searching for the optimal set of values of  $\mathbf{p}^* = [L_p^* \ W_p^* \ x_f^*]$  mm, we define a practical range of values for each parameter as follows:

$$\begin{aligned}
 15.0 \text{ mm} &\leq L_p \leq 40.0 \text{ mm} \\
 15.0 \text{ mm} &\leq W_p \leq 40.0 \text{ mm} \\
 1.0 \text{ mm} &\leq x_f \leq 20.0 \text{ mm}
 \end{aligned}
 \tag{27}$$

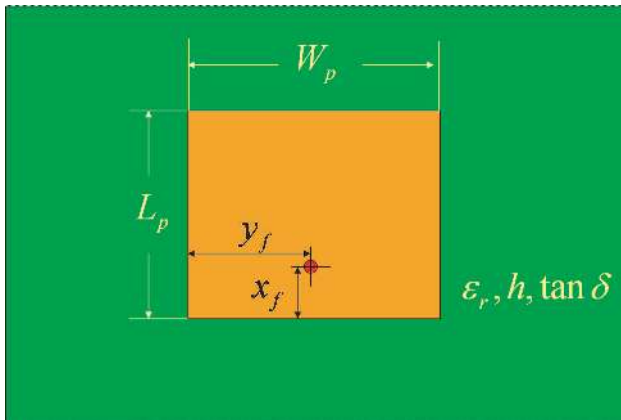


**Figure 12.** The optimizable dimensions of the patch antenna.

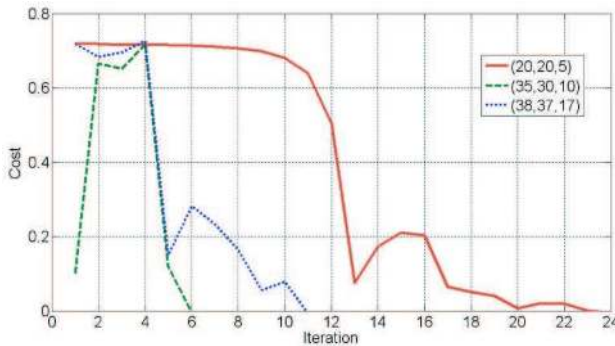


**Figure 13.** Optimization convergence for three different starting points for the patch antenna example.

Next, the algorithm is applied with three different initial guesses: [20.0 20.0 5.0] mm, [35.0 30.0 10.0] mm, and [38.0 37.0 17.0] mm.

The results of running the algorithm for each of these values are shown in Fig. 13. It should be noted that each iteration represents one call to the EM simulator. Table 2 shows the obtained optimal design and the number of iterations for each case. Next, we compare the performance of our approach to that of some of the commonly used commercial optimization packages. We list the results obtained using sequential non-linear, quasi-Newton, and pattern search algorithms. Note that the min-max cost function used in several commercial solvers is a weighted version of that defined in (25). See for example [38] for details on the weighting coefficients. The results when starting optimization from the two arbitrary points [20.0 20.0 5.0] mm and [35.0 30.0 10.0] mm, respectively, are shown in Figs. 14 and 15.

For the first point, the pattern search algorithm converged after 22 calls to the EM simulator. However, none of the algorithms managed to find a design the meets the specifications when using [35.0 30.0 10.0] mm as the starting point.

**Table 2.** Results for the three different cases tested.

Initial Set in mm	Optimal Set in mm	# of Iterations	Cost
[20.0 20.0 5.0]	[34.75 40.0 2.71]	23	-0.0034
[35.0 30.0 10.0]	[34.54 29.62 10.70]	6	-0.0018
[38.0 37.0 17.0]	[34.02 40.0 10.16]	11	-0.0063

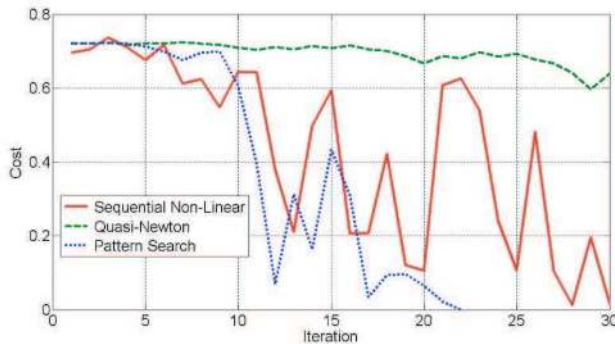


**Figure 14.** Patch antenna optimization convergence using different optimization approaches when starting from the point [20.0 20.0 5.0] mm.

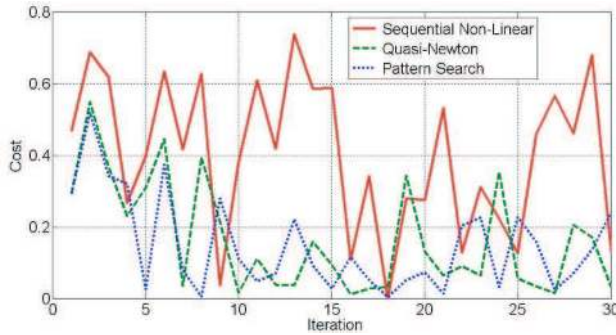


**Figure 15.** Patch antenna optimization convergence using different optimization approaches when starting from the point [35.0 30.0 10.0] mm.

#### 4.2. Multi-objective 4-variable Patch Antenna

Here we apply our algorithm to the design of a global positioning system (GPS) patch antenna. The patch is designed on a rigid foam material with a thickness of 10.0 mm. One basic requirement of this antenna is that it should maintain a  $VSWR \leq 2$  over the bandwidth  $1575 \pm 20$  MHz. In addition, the patch has to be of circular polarization over this band. The following two additional responses are considered:

$$R_{magE} = \frac{||E_{\theta}| - |E_{\varphi}||}{|E_{\theta}| + |E_{\varphi}|} \quad (28)$$

and

$$R_{angE} = |\angle E_{\theta} - \angle E_{\varphi}| \quad (29)$$

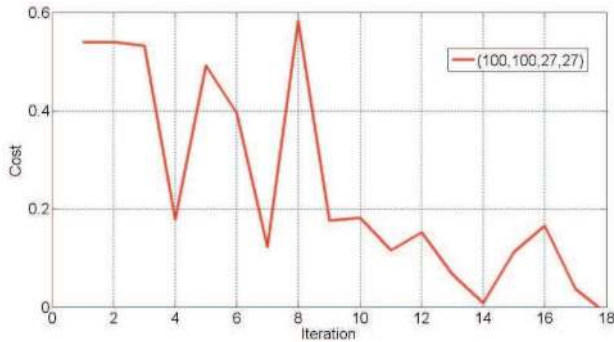
Here, the far field is given by  $\mathbf{E} = E_{\theta}\hat{\theta} + E_{\varphi}\hat{\varphi}$ . To achieve practical circular polarization [42, 43] at a given frequency,  $R_{magE}$  should be less than 0.1, with  $R_{angE} = 90^{\circ} \pm 15^{\circ}$ . Six uniformly distributed in-band frequency points are considered.

The patch variables are the same as those in Fig. 12, but with the feeding probe located at anywhere on the patch. Searching for optimal design of  $\mathbf{p}^* = [L_p^* W_p^* x_f^* y_f^*]$ , we utilize the following practical bounds:

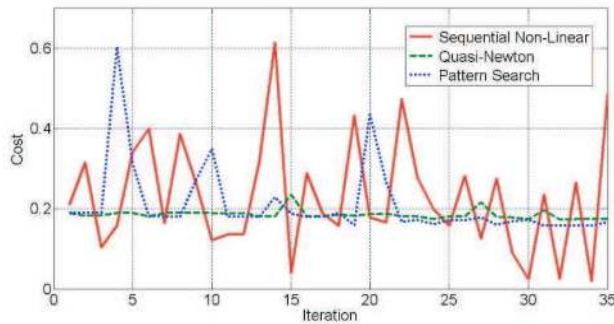
$$\begin{aligned} 50.0 \text{ mm} &\leq L_p \leq 100.0 \text{ mm} \\ 50.0 \text{ mm} &\leq W_p \leq 110.0 \text{ mm} \\ 5.0 \text{ mm} &\leq x_f \leq 30.0 \text{ mm} \\ 5.0 \text{ mm} &\leq y_f \leq 30.0 \text{ mm} \end{aligned} \quad (30)$$

Table 3 shows a summary of results with the convergence shown in Fig. 16. The algorithm converged to a feasible design after 18

calls to the EM simulator. The results obtained when applying other commercially available algorithms are shown in Fig. 17. The optimization stopped after 35 calls to the EM simulator without reaching a feasible design. Figs. 18–20 show the results of the initial and optimized responses of the GPS antenna obtained using our algorithm.



**Figure 16.** Optimization convergence of the GPS antenna design using our algorithm.



**Figure 17.** Optimization convergence of the GPS antenna example using some of the available commercial algorithms.

**Table 3.** Summary of the results for the GPS patch antenna.

Initial Set in mm	Optimal Set in mm	# of Iter.	Cost
[100.0 100.0 27.0 27.0]	[75.4 86.28 13.55 27.21]	18	-0.0414

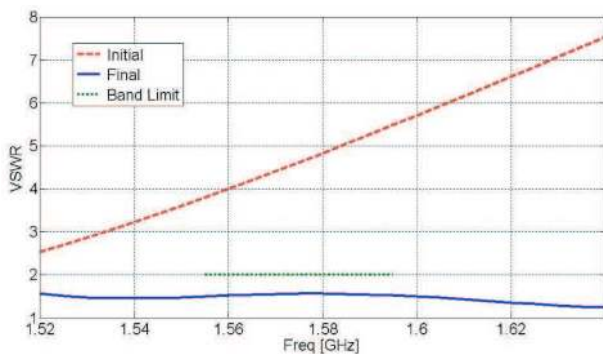


**Figure 18.** The initial and optimized VSWR of the GPS antenna obtained using our algorithm.

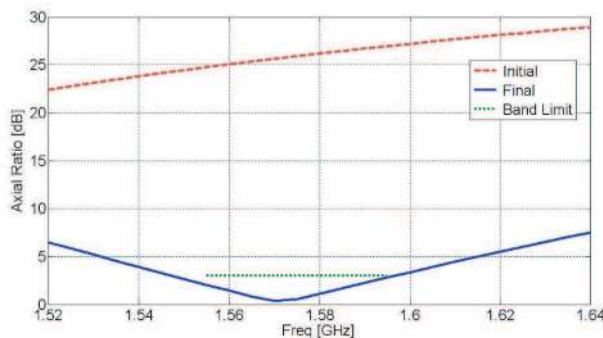


**Figure 19.** The initial and optimized axial ratio of the GPS antenna obtained using our algorithm.

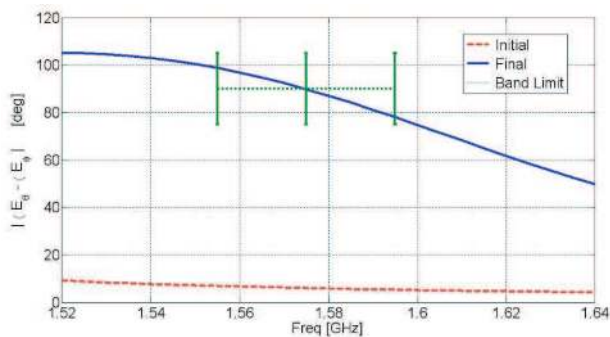


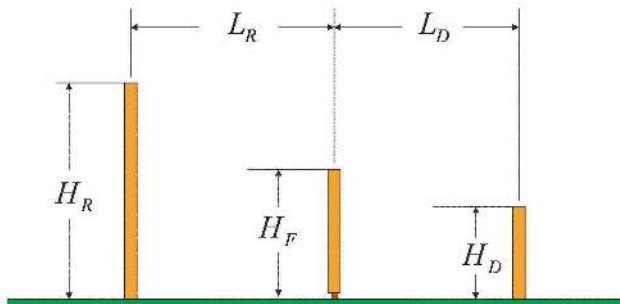
**Figure 20.** The initial and optimized  $|\angle E_{\theta} - \angle E_{\varphi}|$  of the GPS antenna obtained using our algorithm.

### 4.3. A 5-variable Yagi-Uda Antenna

A Yagi-Uda Antenna [42] is a directional antenna system consisting of a feed dipole along with a number of closely coupled parasitic dipole elements (usually a reflector and one or more directors). The design of this antenna has attracted several researchers [44]. Here, we demonstrate the application of our algorithm in designing such an antenna to meet the specifications  $VSWR \leq 2.0$  over the bandwidth 1.5 GHz to 2.5 GHz. For demonstration purposes, we limit the number of directors to only one. In addition, we also do not restrict the out-of-band performance. The diameters of the dipole elements are fixed to 2.1 mm, and are arranged as in Fig. 21. Thus, we have a five dimensional problem with five design variables: The height of the feed dipole element  $H_F$ , the height of the reflector  $H_R$ , the height of the director  $H_D$ , the distance between the reflector and the feed elements  $L_R$ , and the distance between the director and the feed elements  $L_D$ . Ten uniformly distributed in-band frequency points are utilized.

Searching for the optimal design of the parameters  $\mathbf{p}^* = [H_F^* \ L_D^* \ H_D^* \ L_R^* \ H_R^*]$  mm, we impose the following practical parameter ranges:

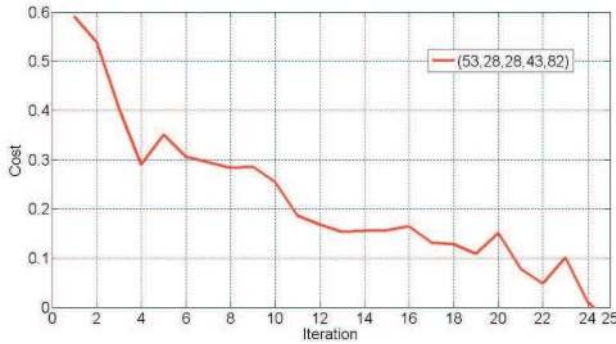
$$\begin{aligned}
 25.0 \text{ mm} &\leq H_F \leq 55.0 \text{ mm} \\
 5.0 \text{ mm} &\leq L_D \leq 30.0 \text{ mm} \\
 10.0 \text{ mm} &\leq H_D \leq 30.0 \text{ mm} \\
 20.0 \text{ mm} &\leq L_R \leq 45.0 \text{ mm} \\
 50.0 &\leq H_R \leq 85.0
 \end{aligned}
 \tag{31}$$



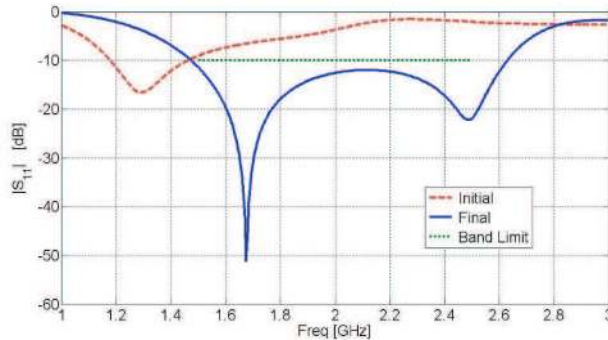
**Figure 21.** The simplified Yagi-Uda example.

**Table 4.** Summary of the results for the Yagi-Uda antenna.

Initial Set in mm	Optimal Set in mm	# of Iter.	Cost
[53.0 28.0 43.0 82.0]	[41.71 9.92 23.7 45 64.44]	25	-0.028



**Figure 22.** Optimization convergence of the Yagi-Uda example using our algorithm.



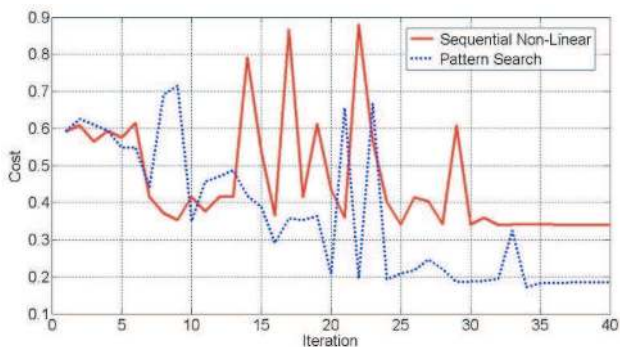
**Figure 23.** The initial and optimized results obtained using our algorithm for the Yagi-Uda example.

Table 4 shows a summary of the results using the proposed algorithm. After 25 calls to the EM simulator, a solution that meets the required specifications is found. The convergence of the algorithm is shown in Fig. 22, with the initial and optimized results shown in Fig. 23. For comparison purposes, commercial optimization tools are utilized as well. The optimization cycle was halted after performing 40 iterations of EM simulations without reaching a solution as shown in Fig. 24.

#### 4.4. Multi-objective 6-variable *E*-slot Antenna

Slot antennas [42, 43] are widely utilized for their high gain and wider bandwidth capabilities as compared to traditional patch antennas. Here, we apply our algorithm to the design of an *E*-slot antenna [45, 46]. This is a multi-objective problem, where the





**Figure 24.** Optimization convergence of the Yagi-Uda example using some of the commercially available algorithms.

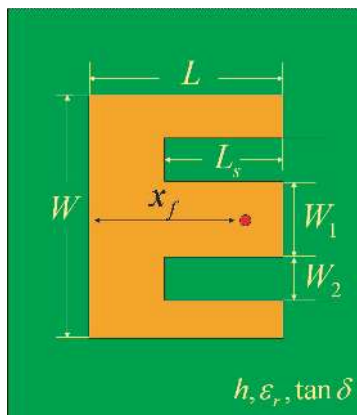


**Figure 25.** The *E*-slot antenna.

desired specifications are  $VSWR \leq 2.0$  and  $gain \geq 8.0$  dBi over the frequency band 1.8 GHz–2.4 GHz. Choosing a foam substrate of 15.0 mm, the *E*-slot patch has six different variables (See Fig. 25) given by  $\mathbf{p}^* = [L^* \ W^* \ L_s^* \ W_1^* \ W_2^* \ x_f^*]$  mm. Here, we impose the limits:

$$\begin{aligned}
 30.0 \text{ mm} &\leq L \leq 70.0 \text{ mm} \\
 30.0 \text{ mm} &\leq W \leq 100.0 \text{ mm} \\
 20.0 \text{ mm} &\leq L_s \leq 70.0 \text{ mm} \\
 4.0 \text{ mm} &\leq W_1 \leq 20.0 \text{ mm} \\
 4.0 \text{ mm} &\leq W_2 \leq 20.0 \text{ mm} \\
 15.0 \text{ mm} &\leq x_f \leq 65.0 \text{ mm}
 \end{aligned}
 \tag{32}$$

Table 5 shows the results for the algorithm, along with the convergence shown in Fig. 26. The required specifications are met after 17 calls to the EM simulator. The initial and optimized impedance and gain bandwidth are shown in Figs. 27 and 28.

**Table 5.** Summary of the results for the slot antenna.

Initial Set in mm	Optimal Set in mm
[65.0 95.0 60.0 18.0 18.0 60.0]	[57.04 92.77 40.57 12.81 14.46 46.09]
# of Iterations	Cost
17	-0.007

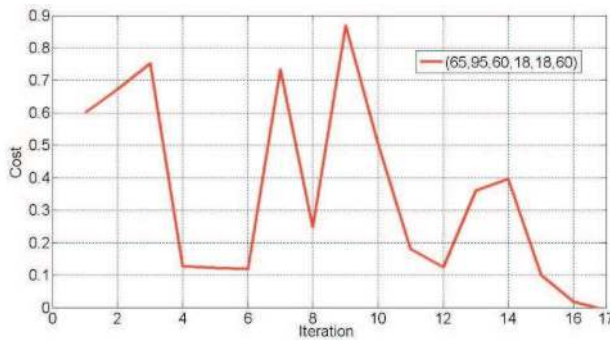


**Figure 26.** Optimization convergence for the *E*-slot antenna obtained using our algorithm.

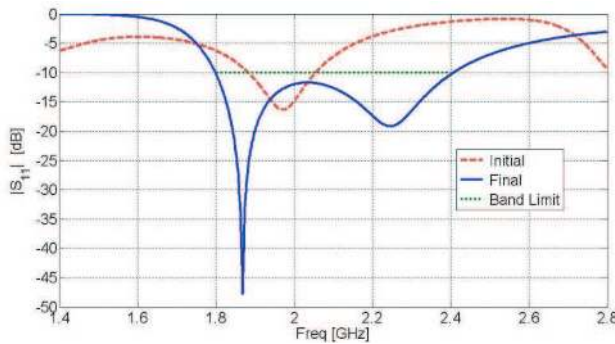


**Figure 27.** The initial and optimized results of the reflection coefficient of the *E*-slot antenna obtained using our algorithm.

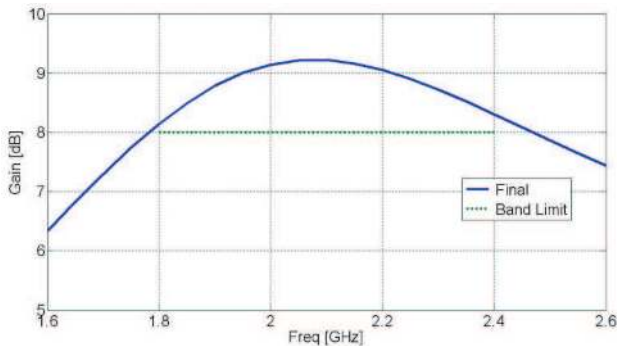


**Figure 28.** The optimized gain of the  $E$ -slot antenna obtained using our algorithm.

## 5. CONCLUSION

We presented a novel on-the-fly optimization algorithm for the optimization of antenna structures. In each iteration, our approach utilizes a surrogate model based on a Cauchy multi-dimensional rational approximation. This approximation is constructed using the available samples obtained during optimization with no prior knowledge or simulations. Our algorithm was successfully used to design several antenna structures with single or multiple objective functions. For the considered structures, the convergence of our approach was shown to be superior to other commercially available optimizers.

## ACKNOWLEDGMENT

The authors would like to thank Ansoft Corporation, COMSOL Group, CST, The Mathworks, Sonnet, and Schmid & Partner Engineering AG for making their software tools available for research at University of Waterloo.

## REFERENCES

1. Preis, K., O. Biro, M. Friedrich, A. Gottvald, and C. Magele, "Comparison of different optimization strategies in the design of electromagnetic devices," *IEEE Transactions on Magnetics*, Vol. 27, No. 5, 4154–4157, Sep. 1991.
2. Ishikawa, T., Y. Tsukui, and M. Matsunami, "Optimization of

- electromagnetic devices using artificial neural network with quasi-Newton algorithm,” *IEEE Transactions on Magnetism*, Vol. 32, No. 3, 1226–1229, May 1996.
3. Yokose, Y., V. Cingoski, and H. Yamashita, “Genetic algorithms with assistant chromosomes for inverse shape optimization of electromagnetic devices,” *IEEE Transactions on Magnetism*, Vol. 36, No. 4, 1052–1056, Jul. 2000.
  4. Villegas, F. J., T. Cwik, Y. Rahmat-Samii, and M. Manteghi, “A parallel electromagnetic genetic-algorithm optimization (EGO) application for patch antenna design,” *IEEE Transactions on Antennas and Propagation*, Vol. 52, No. 9, 2424–2435, Sep. 2004.
  5. Baumgartner, U., C. Magele, K. Preis, and W. Renhart, “Particle swarm optimisation for Pareto optimal solutions in electromagnetic shape design,” *IEE Proceedings on Science, Measurement and Technology*, Vol. 151, No. 6, 499–502, Nov. 2004.
  6. Jin, N. and Y. Rahmat-Samii, “Parallel particle swarm optimization and finite-difference time-domain (PSO/FDTD) algorithm for multiband and wide-band patch antenna designs,” *IEEE Transactions on Antennas and Propagation*, Vol. 53, No. 11, 3459–3468, Nov. 2005.
  7. Jin, N. and Y. Rahmat-Samii, “Advances in particle swarm optimization for antenna designs: Real-number, binary, single-objective and multi-objective implementations,” *IEEE Transactions on Antennas and Propagation*, Vol. 55, No. 3, 556–567, Mar. 2007.
  8. Magele, C. A., K. Preis, W. Renhart, R. Dyczij-Edlinger, and K. R. Richter, “Higher order evolution strategies for the global optimization of electromagnetic devices,” *IEEE Transactions on Magnetism*, Vol. 29, No. 2, 1775–1778, Mar. 1993.
  9. Hoorfar, A., “Evolutionary programming in electromagnetic optimization: A review,” *IEEE Transactions on Antennas and Propagation*, Vol. 55, No. 3, 523–537, Mar. 2007.
  10. Pantoja, M. F., A. R. Bretones, and R. G. Martin, “Benchmark antenna problems for evolutionary optimization algorithms,” *IEEE Transactions on Antennas and Propagation*, Vol. 55, No. 4, 1111–1121, Apr. 2007.
  11. Bandler, J. W., R. M. Biernacki, S. H. Chen, P. A. Grobelny, and Y. Shen, “Yield driven electromagnetic optimization via multilevel multidimensional models,” *IEEE Transactions on Microwave Theory and Techniques*, Vol. 41, No. 12, 2269–2278, Dec. 1993.
  12. Bandler, J. W., R. M. Biernacki, S. H. Chen, P. A. Grobelny, and R. H. Hemmers, “Space mapping technique for electromagnetic

- optimization,” *IEEE Transactions on Microwave Theory and Techniques*, Vol. 42, No. 12, Part 1, 2536–2544, Dec. 1994.
13. Bandler, J. W., R. M. Biernacki, S. H. Chen, P. A. Grobelny, R. H. Hemmers, and K. Madsen, “Electromagnetic optimization exploiting aggressive space mapping,” *IEEE Transactions on Microwave Theory and Techniques*, Vol. 43, No. 12, 2874–2882, Dec. 1995.
  14. Bakr, M. H., J. W. Bandler, R. M. Biernacki, S. H. Chen, and K. Madsen, “A trust region aggressive space mapping algorithm for EM optimization,” *IEEE Transactions on Microwave Theory and Techniques*, Vol. 46, No. 12, 2412–2425, Dec. 1998.
  15. Bakr, M. H., J. W. Bandler, N. Georgieva, and K. Madsen, “A hybrid aggressive space-mapping algorithm for EM optimization,” *IEEE Transactions on Microwave Theory and Techniques*, Vol. 47, No. 12, 2440–2449, Dec. 1999.
  16. Hoole, S. R. H. and M. K. Haldar, “Optimization of electromagnetic devices: Circuit models, neural networks and gradient methods in concert,” *IEEE Transactions on Magnetics*, Vol. 31, No. 3, 2016–2019, May 1995.
  17. Mohammed, O. A., D. C. Park, and F. G. Uler, “Design optimization of electromagnetic devices using artificial neural networks,” *IEEE Transactions on Magnetics*, Vol. 28, No. 5, 2805–2807, Sep. 1992.
  18. Hawe, G. and J. Sykulski, “Considerations of accuracy and uncertainty with kriging surrogate models in single-objective electromagnetic design optimization,” *IET on Science, Measurement & Technology*, Vol. 1, No. 1, 37–47, Jan. 2007.
  19. Koziel, S. and J. W. Bandler, “Space-mapping optimization with adaptive surrogate model,” *IEEE Transactions on Microwave Theory and Techniques*, Vol. 55, No. 3, 541–547, Mar. 2007.
  20. Bakr, M. H., J. W. Bandler, K. Madsen, J. E. Rayas-Sanchez, and J. Sondergaard, “Space-mapping optimization of microwave circuits exploiting surrogate models,” *IEEE Transactions on Microwave Theory and Techniques*, Vol. 48, No. 12, 2297–2306, Dec. 2000.
  21. Adve, R. S., T. K. Sarkar, S. M. Rao, E. K. Miller, and D. R. Pflug, “Application of the Cauchy method for extrapolating/interpolating narrow-band system responses,” *IEEE Transactions on Microwave Theory and Techniques*, Vol. 45, 837–845, May 1997.
  22. Kottapalli, K., T. K. Sarkar, Y. Hua, E. K. Miller, and G. J. Burke, “Accurate computation of wide-band response

- of electromagnetic systems utilizing narrow-band information," *IEEE Transactions on Microwave Theory and Techniques*, Vol. 39, 682–687, Apr. 1991.
23. Appiah, R., "Cauchy interpolation in linear system reduction," *IEEE Transactions on Automatic Control*, Vol. 22, No. 6, 974–976, Dec. 1977.
  24. Peik, S. F., R. R. Mansour, and Y. L. Chow, "Multidimensional Cauchy method and adaptive sampling for an accurate microwave circuit modeling," *IEEE Transactions on Microwave Theory and Techniques*, Vol. 46, No. 12, 2364–2371, Dec. 1998.
  25. De Geest, J., T. Dhaene, N. Fache, and D. De Zutter, "Adaptive CAD-model building algorithm for general planar microwave structures," *IEEE Transactions on Microwave Theory and Techniques*, Vol. 47, No. 9, 1801–1809, Sep. 1999.
  26. Lehmensiek, R. and P. Meyer, "Creating accurate multivariate rational interpolation models of microwave circuits by using efficient adaptive sampling to minimize the number of computational electromagnetic analyses," *IEEE Transactions on Microwave Theory and Techniques*, Vol. 49, No. 8, 1419–1430, Aug. 2001.
  27. Lamecki, A., P. Kozakowski, and M. Mrozowski, "Efficient implementation of the Cauchy method for automated CAD-model construction," *IEEE Microwave and Wireless Components Letters*, Vol. 13, No. 7, 268–270, Jul. 2003.
  28. Cuyt, A., R. B. Lenin, S. Becuwe, and B. Verdonk, "Adaptive multivariate rational data fitting with applications in electromagnetics," *IEEE Transactions on Microwave Theory and Techniques*, Vol. 54, No. 5, 2265–2274, May 2006.
  29. Shaker, G. S. A., M. H. Bakr, N. Sangary, and S. Safavi-Naeini, "Space mapping-based optimization exploiting tolerant Cauchy approximations," *IEEE International Microwave Symposium*, Jun. 2009.
  30. Bertsekas, D. P., *Nonlinear Programming*, Athena Scientific, Belmont, Massachusetts, 1995.
  31. Boyd, S. and L. Vandenberghe, *Convex Optimization*, Cambridge University Press, 2004.
  32. Mosek 5.0.0.93, Mosek ApS, 2008, Available: [www.mosek.com](http://www.mosek.com).
  33. TOMLAB v6.1, Tomlab Optimization, 2008, Available: [www.tomopt.com](http://www.tomopt.com).
  34. MATLAB R2008a, The MathWorks, 2008, Available: [www.mathworks.com](http://www.mathworks.com).
  35. Koh, C. S., S. Y. Hahn, T. K. Chung, and H. K. Jung, "A

- sensitivity analysis using boundary element method for shape optimization of electromagnetic devices,” *IEEE Transactions on Magnetism*, Vol. 28, No. 2, 1577–1580, Mar. 1992.
36. Ansoft Designer v3.5, Ansoft, LLC, 2008, Available: [www.ansoft.com/products/hf/ansoft\\_designer/](http://www.ansoft.com/products/hf/ansoft_designer/).
  37. Ansoft HFSS v11.0, Ansoft, LLC, 2008, Available: [www.ansoft.com/products/hf/hfss/](http://www.ansoft.com/products/hf/hfss/).
  38. COMSOL MULTIPHYSICS v3.4, COMSOL Group, 2008, Available: [www.comsol.com](http://www.comsol.com).
  39. CST Microwave Studio 2008, CST, 2008, Available: [www.cst.com](http://www.cst.com).
  40. Sonnet v11.0, Sonnet, 2008, Available: [www.sonnetusa.com](http://www.sonnetusa.com).
  41. SEMCAD 13.4 Bernina, Schmid & Partner Engineering AG, 2008, Available: [www.semcad.com](http://www.semcad.com).
  42. Balanis, C. A., *Antenna Theory: Analysis and Design*, 3rd Edition, Wiley-Interscience, 2005.
  43. Garg, R., P. Bhartia, I. Bahl, and A. Ittipiboon, *Microstrip Antenna Design Handbook*, Artech House, Boston, USA, 2001.
  44. Misra, I. S., R. S. Chakrabarty, and B. B. Mangaraj, “Design, analysis and optimization of V-dipole and its three-element Yagi-Uda array,” *Progress In Electromagnetics Research*, PIER 66, 137–156, 2006.
  45. Kumar, G. and K. P. Ray, *Broadband Microstrip Antennas*, Artech House, Boston, USA, 2003.
  46. Ang, B.-K. and B.-K. Chung, “A wideband E-shaped microstrip patch antenna for 5–6 GHz wireless communications,” *Progress In Electromagnetics Research*, PIER 75, 397–407, 2007.